



Article

# Radical in the Peroxide-Produced F-Type Ferryl Form of Bovine Cytochrome *c* Oxidase

Tereza Sztachova<sup>1</sup>, Adriana Tomkova<sup>1</sup>, Erik Cizmar<sup>2</sup> , Daniel Jancura<sup>1,\*</sup> and Marian Fabian<sup>3,\*</sup>

<sup>1</sup> Department of Biophysics, Faculty of Science, University of P. J. Safarik, Jesenna 5, 041 54 Kosice, Slovakia

<sup>2</sup> Department of Condensed Matter Physics, Faculty of Science, University of P. J. Safarik, Park Angelinum 9, 040 01 Kosice, Slovakia

<sup>3</sup> Center for Interdisciplinary Biosciences, Technology and Innovation Park, University of P. J. Safarik, Jesenna 5, 041 54 Kosice, Slovakia

\* Correspondence: daniel.jancura@upjs.sk (D.J.); marian.fabian@upjs.sk (M.F.)

**Abstract:** The reduction of O<sub>2</sub> in respiratory cytochrome *c* oxidases (CcO) is associated with the generation of the transmembrane proton gradient by two mechanisms. In one of them, the proton pumping, two different types of the ferryl intermediates of the catalytic heme *a*<sub>3</sub>-Cu<sub>B</sub> center **P** and **F** forms, participate. Equivalent ferryl states can be also formed by the reaction of the oxidized CcO (**O**) with H<sub>2</sub>O<sub>2</sub>. Interestingly, in acidic solutions a single molecule of H<sub>2</sub>O<sub>2</sub> can generate from the **O** an additional F-type ferryl form (**F**<sup>•</sup>) that should contain, in contrast to the catalytic **F** intermediate, a free radical at the heme *a*<sub>3</sub>-Cu<sub>B</sub> center. In this work, the formation and the endogenous decay of both the ferryl iron of heme *a*<sub>3</sub> and the radical in **F**<sup>•</sup> intermediate were examined by the combination of four experimental approaches, isothermal titration calorimetry, electron paramagnetic resonance, and electronic absorption spectroscopy together with the reduction of this form by the defined number of electrons. The results are consistent with the generation of radicals in **F**<sup>•</sup> form. However, the radical at the catalytic center is more rapidly quenched than the accompanying ferryl state of heme *a*<sub>3</sub>, very likely by the intrinsic oxidation of the enzyme itself.



**Citation:** Sztachova, T.; Tomkova, A.; Cizmar, E.; Jancura, D.; Fabian, M. Radical in the Peroxide-Produced F-Type Ferryl Form of Bovine Cytochrome *c* Oxidase. *Int. J. Mol. Sci.* **2022**, *23*, 12580. <https://doi.org/10.3390/ijms232012580>

Academic Editor: Larry Fliegel

Received: 14 September 2022

Accepted: 18 October 2022

Published: 20 October 2022

**Publisher's Note:** MDPI stays neutral with regard to jurisdictional claims in published maps and institutional affiliations.



**Copyright:** © 2022 by the authors. Licensee MDPI, Basel, Switzerland. This article is an open access article distributed under the terms and conditions of the Creative Commons Attribution (CC BY) license (<https://creativecommons.org/licenses/by/4.0/>).

**Keywords:** cytochrome oxidase; free radical; ferryl intermediate; electron paramagnetic resonance spectroscopy; isothermal titration calorimetry

## 1. Introduction

The final step of cellular respiration in aerobic organisms is the reduction of O<sub>2</sub> to H<sub>2</sub>O catalyzed mainly by the membrane-bound heme-copper oxidases. Cytochrome *c* oxidases (CcO), the large subclass of heme-copper oxidases, are found in all mitochondria and some types of bacteria [1]. The reduction of oxygen in CcO is accomplished by electrons accepted from ferrocytochrome *c* (c<sup>2+</sup>). The electron transfer from c<sup>2+</sup> to O<sub>2</sub> is facilitated by four redox centers of CcO: Cu<sub>A</sub>, iron of heme *a* (Fe<sub>a</sub>), iron of heme *a*<sub>3</sub> (Fe<sub>a3</sub>), and Cu<sub>B</sub>. A dinuclear copper center, Cu<sub>A</sub>, is the first acceptor of electrons from c<sup>2+</sup>. These electrons are rapidly distributed between Cu<sub>A</sub> and Fe<sub>a</sub> [2–4]. The intraprotein flow of electrons then continues from Fe<sub>a</sub> to the catalytic binuclear Fe<sub>a3</sub>-Cu<sub>B</sub> center where the reduction of O<sub>2</sub> to H<sub>2</sub>O occurs (Figure 1). The catalytic center is also the site where the inhibitors (e.g., cyanide, azide, CO) of CcO can be bound.

The reduction of O<sub>2</sub> in CcO proceeds via several distinct oxy-intermediates determined by the number of electrons and protons accepted by the catalytic Fe<sub>a3</sub>-Cu<sub>B</sub> center (Figure 2) (for reviews [5–10]). From these intermediates, the most important and intriguing are the ferryl states that are divided, based on their optical spectra, into the **P** (**P<sub>M</sub>**, **P<sub>R</sub>**) and the **F** (**F**, **F**<sup>•</sup>)-type forms.

The **P<sub>M</sub>** is produced by the reaction of two-electron reduced (mixed-valence) CcO with O<sub>2</sub> [11–15]. It was named **P<sub>M</sub>** since originally it was expected to have a peroxide bound at the catalytic center (e.g., Fe<sub>a3</sub><sup>3+</sup>-O-O-Cu<sub>B</sub><sup>2+</sup>). However, it has been shown later that the

dioxygen bond in this intermediate is already cleaved by a four-electron reduction of  $O_2$ . Two of them are coming from the oxidation of  $Fe_{a_3}^{2+}$  to  $Fe_{a_3}^{4+}=O$ , one from the oxidation of  $Cu_B^+$  to  $Cu_B^{2+}$ , and the donor of the fourth electron is plausibly the nearby Tyr244 (bovine CcO numbering), producing the free radical ( $YO^\bullet$ ) at the vicinity of the catalytic center (Figures 1 and 2).

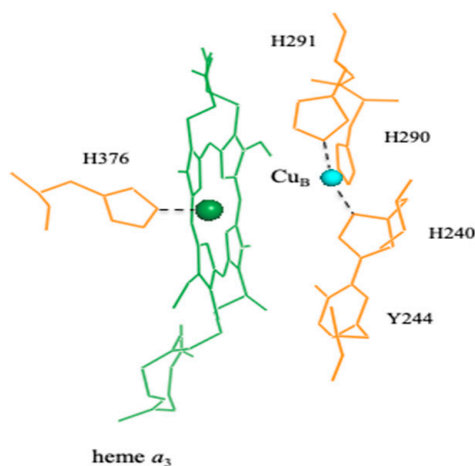


**Figure 1.** Structure of the catalytic heme  $a_3$ - $Cu_B$  center of bovine cytochrome  $c$  oxidase. His376 is bound to the iron of heme  $a_3$  (green sphere).  $Cu_B$  (cyan sphere) is coordinated by His291, His290 and His240. A covalent bond is present between His240 and Tyr244 (PDB. ID: 1V54).

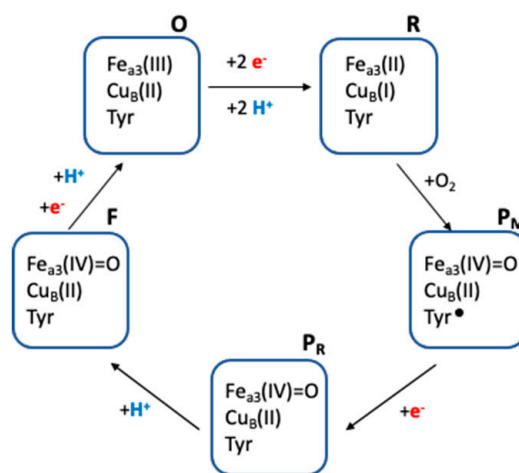


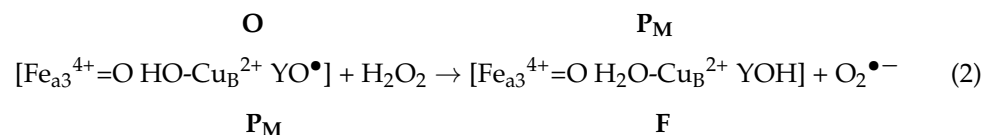
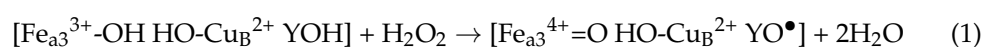
**Figure 2.** Abbreviated catalytic cycle of CcO illustrating a sequential formation of the ferryl intermediates of the catalytic heme  $a_3$ - $Cu_B$  center during the reaction of the reduced enzyme with  $O_2$ .

Delivery of the third electron into the catalytic site of  $P_M$  leads to the appearance of the second  $P$ -type intermediate, the  $P_R$  (Figure 2). Since the radical is reduced in this intermediate and the visible absorption spectrum is almost identical to  $P_M$  it was named  $P_R$  [12,16–19]. A characteristic feature of these intermediates is a sharp  $\alpha$ -band with a maximum at 607 nm in the difference spectra of  $P_M$  and  $P_R$  relative to the oxidized CcO.

One proton uptake into the catalytic center of the  $P_R$  triggers the  $P_R$ -to- $F$  transition (Figure 2). This conversion is connected with the change in both the shape and the maximum of the  $\alpha$ -band that is shifted from 607 to 580 nm [20–28]. With the transfer of an additional electron and proton into the  $F$  intermediate, the reduction of  $O_2$  to water is completed and the oxidized CcO ( $O$ ) is recovered [20–26,29–35].

Analogous ferryl states can be produced by the reaction of the oxidized CcO with hydrogen peroxide as well [36–41]. Interestingly, the reaction of the  $O$  with peroxide can generate two types of the  $F$  form ( $F$ ,  $F^\bullet$ ). The peroxide-produced  $F$  state should be

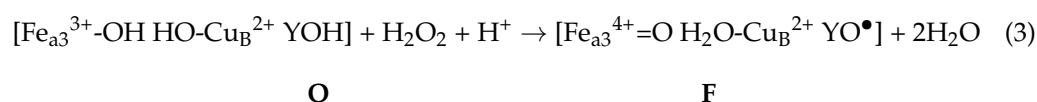
equivalent to the catalytic intermediate. Its formation by two molecules of H<sub>2</sub>O<sub>2</sub> can be pictured by these two reactions:



where the first molecule of H<sub>2</sub>O<sub>2</sub> produces the P<sub>M</sub> form [37,39,42–44] and the second peroxide is expected to reduce the YO<sup>•</sup> and generate the F state and release the superoxide [38,45].

The conversion of the P form to the F state is not restricted only to the proton uptake. It has been proposed several times that in the transition from P to F form the structural change should also participate [15,46]. Importantly, the recent crystallographic data indicated that the difference between these two ferryl forms is in the slight variance of the axial coordination of Fe<sup>4+</sup> [47].

Interestingly, another F-type ferryl form (F<sup>•</sup>) is possible to prepare by reacting the O with one molecule of H<sub>2</sub>O<sub>2</sub> in acidic buffers [37,39,43]. Based on the nature of the reaction and the apparent proton uptake into the Fe<sub>a3</sub>-Cu<sub>B</sub> center during this process [39,43], the production of the F<sup>•</sup> may be illustrated by this scheme:



Small differences between the F<sup>•</sup> (a dot underline the radical present at the catalytic site of CcO) and the F intermediates in UV-Vis absorption spectra may indicate the distinct redox state of the catalytic center in these two ferryl states [37,39,43,48–50]. Particularly, the position of the maxima of the α-band at 575 and 580 nm are observed in the difference spectra of the F<sup>•</sup> and the F vs. the O, respectively.

Several previous studies, employing the electron paramagnetic resonance (EPR), uncovered multiple radicals in the peroxide-generated ferryl forms of CcO, however, showing low and variable yields [37,51–54]. Moreover, the correlation between the amount of the detected radicals and the concentration of the F<sup>•</sup> form of the bovine CcO has not been established, yet [51,53,54]. In addition, some earlier works indicated the migration of the primary radical a large distance from the heme a<sub>3</sub>-Cu<sub>B</sub> center [55–59]. When the oxidized enzyme was reacted with an excess of H<sub>2</sub>O<sub>2</sub>, the oxidative modification of the distant tryptophan residues and the bound phospholipids together with the spin trapping of the radical at the surface of purified CcO has been observed [55–59].

In this study, the formation of the radical in the F<sup>•</sup> state of the purified bovine CcO was verified and its lifetime at the catalytic center was examined. The data obtained by the application of four different experimental approaches support the production of the radical at the catalytic center in the F<sup>•</sup> form. However, autoxidation of CcO triggers the quenching of this primary radical with a rate that should be at least ten times faster (time constant of τ ≤ 9 s) than the rate of the spectral development (τ ≈ 90 s) of the ferryl state of heme a<sub>3</sub> (Fe<sub>a3</sub><sup>4+</sup>=O) (pH 5.7, 5 °C). The data also showed that the small spectral differences between the F<sup>•</sup> and the F states do not indicate the distinct redox state of the catalytic center in these ferryl forms.

## 2. Results

In all measurements, the F<sup>•</sup> intermediate was produced by the reaction of the oxidized CcO (O) with either sub- or stoichiometric amount of H<sub>2</sub>O<sub>2</sub> in an acidic buffer at pH 5.7 and 5 °C. The formation of F<sup>•</sup> and its endogenous conversion to the O was monitored by a combination of isothermal titration calorimetry (ITC), UV-Vis absorption, and EPR spectroscopies.

### 2.1. Formation and Decay of $F^\bullet$ Form—UV-Vis and ITC Measurements

The production of the  $F^\bullet$  state by the reaction of the oxidized CcO ( $49 \mu\text{M}$ ) with a sub-stoichiometric amount of  $\text{H}_2\text{O}_2$  ( $5.4 \mu\text{M}$ ) ( $\text{O} + \text{H}_2\text{O}_2 \rightarrow \text{F}^\bullet$ ) is shown in Figure 3. The kinetics of the formation of this state followed by its spontaneous transition to the  $\text{O}$  form were registered using the change of the absorbance  $\Delta A$  (575–630 nm) (Figure 3A). After the addition of peroxide, the production of the  $F^\bullet$ , represented by the rise of  $\Delta A$  (575–630 nm), is completed in  $\sim 600$  s. The subsequent decline of the absorbance is due to the endogenous decay of the  $F^\bullet$ -to- $\text{O}$  state. From the two-exponential fit of this kinetics, the time constants of  $\sim 80$  s and  $\sim 3 \times 10^3$  s were attained for the generation and the decomposition of the  $F^\bullet$ , respectively.

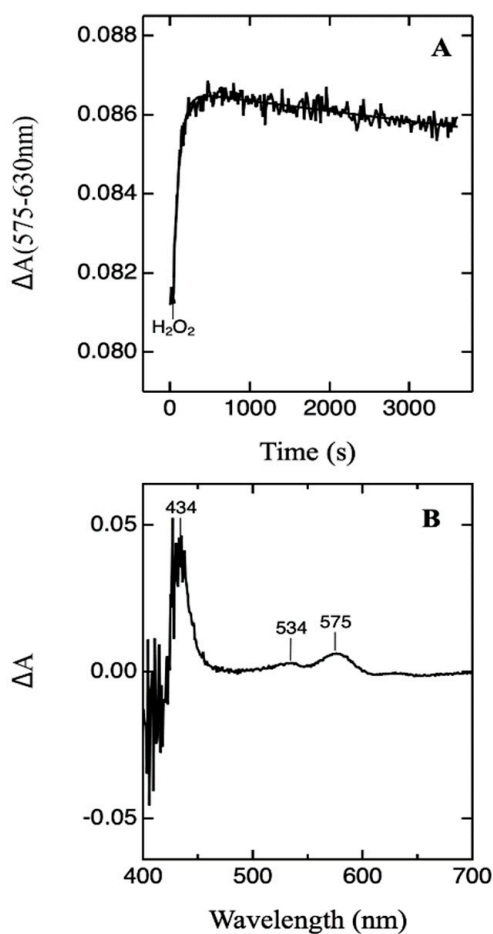


**Figure 3.** Production of the ferryl  $F^\bullet$  state of cytochrome oxidase by  $\text{H}_2\text{O}_2$ . (A) The kinetics of the formation of the  $F^\bullet$  intermediate by the reaction of the oxidized CcO ( $49 \mu\text{M}$ ) with  $\text{H}_2\text{O}_2$  ( $5.4 \mu\text{M}$ ) at  $5^\circ\text{C}$  and its subsequent endogenous decay registered by the absorbance change  $\Delta A$  (575–630 nm). The arrow ( $\text{H}_2\text{O}_2$ ) shows the time of peroxide injection. (B) The difference spectrum obtained after the subtraction of the spectrum of the initial oxidized CcO from the spectrum collected at the time (600 s) when the absorption change  $\Delta A$  (575–630 nm) reached the maximum. The arrow ( $\text{H}_2\text{O}_2$ ) shows the time of peroxide injection. The buffer was 39 mM potassium phosphate, pH 5.7, 12.5 mM  $\text{K}_2\text{SO}_4$ , 0.6% DM and superoxide dismutase (30 units/mL).

The production of the  $F^\bullet$  state is shown by the difference spectrum,  $F^\bullet$  versus  $\text{O}$  ( $F^\bullet$ - $\text{O}$ ), exhibiting the characteristic maxima at 575, 534, and  $\sim 435$  nm and the minimum at  $\sim 412$  nm (Figure 3B). The spectrum was collected at the time when the maximal amount of the ferryl form was formed (600 s). The average amount of the  $F^\bullet$  produced by a single molecule of  $\text{H}_2\text{O}_2$  was found to be  $1.02 \pm 0.07$  ( $n = 3$ ).

A large noise in the difference spectrum in the region of the Soret band (400–450 nm) is a consequence of the high absorbance in this region (ca. 1.5). In the absolute spectrum, this

band exhibits the maximum at  $\sim 423$  nm for the oxidized CcO and is slightly red-shifted ( $\sim 424$  nm) after the reaction with peroxide.

The heat changes associated with this reaction are illustrated in Figure 4 ( $F^\bullet$ , full line). The negative values of the time dependence of the power demonstrate that heat is released in this reaction. The maximum rate of heat release is observed at the beginning of the reaction initiated by the peroxide injection (Figure 4,  $H_2O_2$  arrow). At about 600 s, when the formation of the  $F^\bullet$  is spectrally completed, this rate is nearly zero. From the integration of the area under the ITC curves, the average reaction enthalpy change  $\Delta H = -39.2 \pm 0.7$  kcal/mol  $H_2O_2$  ( $n = 3$ ) was obtained.

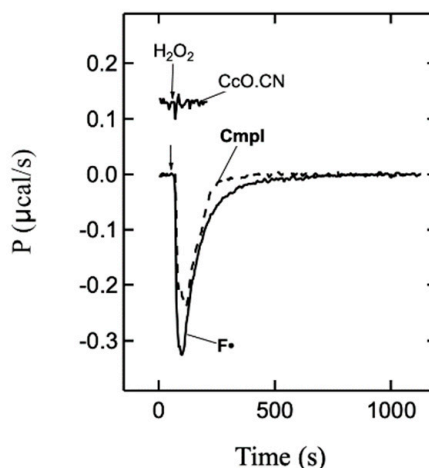


**Figure 4.** Heat released during the production of the  $F^\bullet$  state. The time dependence of the rate of the heat release following the injection of peroxide ( $5 \mu\text{M}$ ) into the reaction cell filled with  $50 \mu\text{M}$  oxidized native CcO ( $F^\bullet$  full line),  $50 \mu\text{M}$  CN-ligated oxidized CcO (CcO.CN line) and  $5 \mu\text{M}$  horseradish peroxidase (CmpI, dashed line) at  $5^\circ\text{C}$ . The arrows ( $H_2O_2$ ) show the time of peroxide injection. The buffer was  $39$  mM potassium phosphate, pH  $5.7$ ,  $12.5$  mM  $K_2SO_4$ , and superoxide dismutase ( $30$  units/mL). The buffer with CcO samples also contained  $0.6\%$  DM.

Control ITC measurements during the reaction of  $50 \mu\text{M}$  CN-ligated CcO with  $5 \mu\text{M}$   $H_2O_2$  demonstrate that there is a negligible contribution of possible side reactions (Figure 4, CcO.CN line). In this case, the heat released is about  $2\%$  of the value of  $\Delta H$  obtained for the uninhibited CcO. This heat was subtracted from the measured value of  $\Delta H$ .

A similar ferryl state of heme, the compound I ( $Fe^{4+}=O \pi^{\bullet+}$ ), can be generated by reacting the oxidized horseradish peroxidase (HRP) with the stoichiometric amount of  $H_2O_2$  (Figure 4, cmpI dashed line). The advantage of this measurement is that the presence and stability of both the ferryl iron and the  $\pi$  cation radical can be simply monitored by the optical spectrum [60,61]. The obtained spectra showed that the reaction of  $5 \mu\text{M}$  of the oxidized HRP with  $5 \mu\text{M}$   $H_2O_2$  produces in mixing time ( $\sim 10$  s) a stable compound I at pH  $5.7$  and  $5^\circ\text{C}$ . The enthalpy change  $\Delta H$  of  $-27.1 \pm 1.8$  kcal/mol  $H_2O_2$  ( $n = 3$ ) was associated with this reaction. In the determination of the reaction  $\Delta H$ , the heats of dilution and mixing were subtracted.

## 2.2. Formation of Radical in the $F^\bullet$ State—UV-Vis and EPR Measurements

The production of the  $F^\bullet$  state and its endogenous transition to the  $O$  was registered by the parallel measurements of its visible absorption and EPR spectra. The time dependence of the formation and decay of  $F^\bullet$ ,  $P_M$ , and radical ( $R^\bullet$ ) observed by EPR spectroscopy in the reaction of  $98 \mu\text{M}$   $O$  with  $98 \mu\text{M}$   $H_2O_2$  is presented in Figure 5. The time dependencies of the relative amount of  $F^\bullet$ ,  $P_M$ , and  $R^\bullet$  versus the total concentration of the  $O$ , are shown for the time period of  $6 \times 10^3$  s. The maximum amount of the  $F^\bullet$  is observed in  $\sim 1000$  s after the addition of peroxide to the  $O$  state (Figure 5A, F). The appearance of the  $F^\bullet$  form is, however, attained in two different kinetic phases. The first and major phase is completed in  $\sim 120$  s ( $70\%$ ) and is characterized by a time constant of  $\sim 26$  s. The next slower phase

is described by  $\tau = \sim 330$  s (30%) (Table 1). Subsequently, the much slower endogenous transition of the  $F^\bullet$ -to- $O$  state proceeds with  $\tau = 2.9 \times 10^4$  s.

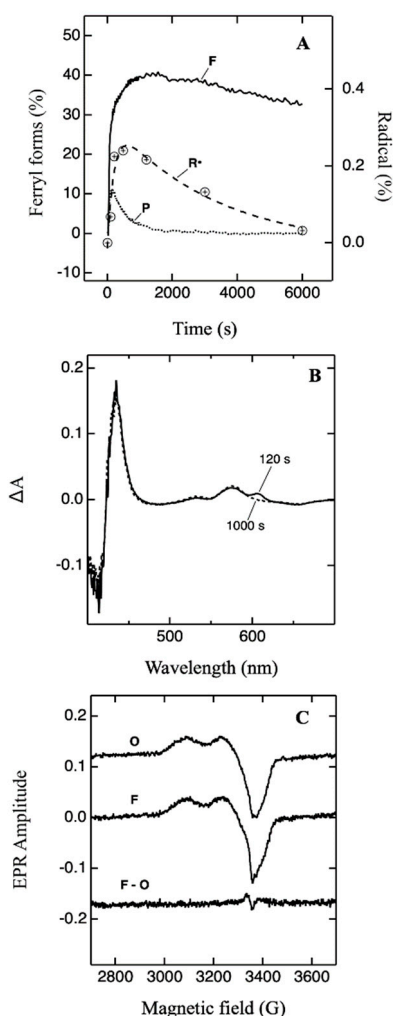


**Figure 5.** Production and decay of ferryl intermediates and the radical registered by visible absorption and EPR spectroscopies. (A) Kinetics of the generation and the endogenous decay of the  $F^\bullet$  (F, full line), the  $P_M$  (P, dotted line), and the radical ( $R^\bullet$ , dashed line) observed during the reaction of  $98 \mu\text{M}$  oxidized CcO with  $98 \mu\text{M}$   $\text{H}_2\text{O}_2$  at pH 5.7 and  $5^\circ\text{C}$ . (B) The difference spectra of peroxide-treated CcO collected at 120 s (full line) and 1000 s (dashed line) after the injection of  $\text{H}_2\text{O}_2$  vs. initial oxidized CcO. (C) The corresponding EPR spectra of initial oxidized CcO (O), the peroxide-treated CcO at 1200 s (F), and the difference between these two spectra (F-O). The spectra were collected at 80 K using a power of 0.2 mW (for details see Materials and Methods). The amount of ferryl intermediates and the radical is expressed relative to the total concentration of CcO. Buffer: 101 mM KPi, 30 mM  $\text{K}_2\text{SO}_4$ , 0.6% DM and 260 units/mL SOD.

**Table 1.** Time constants ( $\tau$ ) of the generation of ferryl intermediates and the free radical during the reaction of the oxidized CcO ( $98 \mu\text{M}$ ) with hydrogen peroxide ( $98 \mu\text{M}$ ) at pH 5.7 and  $5^\circ\text{C}$ .

Reaction	$\tau$ (s)
rapid formation of $F^\bullet$	26
formation of $P_M$	22
loss of $P_M$	330
slow formation of $F^\bullet$	330
formation of the radical	200

At the same time, the transient appearance of a small fraction of the  $P_M$  state is also detected in this sample (Figure 5A,  $P_M$  dotted line). The time constant of this phase,  $\sim 22$  s, is close to the rate of the rapid phase of the formation of the  $F^\bullet$ . The disappearance of the  $P_M$  occurs with the same time constant of  $\sim 330$  s as the rate of the generation of the  $F^\bullet$  in the slow phase (Table 1).

The difference in visible spectra also demonstrates the initial rapid appearance of the  $P_M$  state (Figure 5B). This form is distinguished by the band having the maximum at 607 nm in the spectrum registered 120 s after the initiation of the reaction (Figure 5B, 120 s full line). This band at 607 nm then disappears and only a single band with the maximum at 575 nm is present (1000 s after injection of peroxide, dashed line).

The radical in the EPR spectra appear with the time constant of  $\tau = \sim 200$  s followed by its much slower disappearance ( $\tau = \sim 3300$  s) (Figure 5A,  $R^\bullet$  dashed line). However, its maximal yield, calculated relative to the EPR signal of  $Cu_A^{2+}$ , is only about 0.2% of the used CcO (0.6% relative to the formed  $F^\bullet$ ) (Figure 5C). This is documented by the EPR spectra of the initial  $O$  and the  $F^\bullet$  forms collected on the sample frozen in 1200 s after the peroxide addition. The spectrum of the radical (Figure 5C,  $F-O$ ) was obtained by the subtraction of the spectrum of the  $O$  from the  $F^\bullet$  state. The radical is characterized by  $g = 2.005$  and the linewidth of  $\sim 28$  G.

### 2.3. One-Electron Reduction of the $F^\bullet$ Form

The redox state of the catalytic center of CcO in the  $F^\bullet$  state was examined by the reduction with the substoichiometric amount of one-electron donor to minimize more than one electron transfer into the catalytic center of CcO. The formation of the  $F^\bullet$  state and its reduction by ferrocyanide under aerobic conditions are shown in Figure 6. At the time of the addition of catalase (Figure 6A, cat arrow), 300 s after the peroxide injection, the interaction of the  $O$  (50  $\mu$ M) with the substoichiometric concentration of  $H_2O_2$  (48  $\mu$ M) resulted in the formation of 19.3  $\mu$ M  $F^\bullet$  (39%) with the kinetics characterized by  $\tau = \sim 90$  s.

Into this sample, containing 19.3  $\mu$ M  $F^\bullet$  and 30.7  $\mu$ M  $O$ , the sub-stoichiometric amount of potassium ferrocyanide (9.9  $\mu$ M, final concentration) was injected as indicated by the second arrow (Figure 6A,  $Fe^{2+}$  arrow). The injection of the electron donor triggers a rapid disappearance of the  $F^\bullet$  displayed as the fast decrease of  $\Delta A$  (575–630 nm) (Figure 6A) followed by a slow endogenous transition of the  $F^\bullet$ -to- $O$ .

The difference between the spectrum collected before and 500 s after the addition of ferrocyanide ( $Fe^{2+}$ ) revealed that in this sample some small fraction of the  $P_M$  is also present. The reduction of these two ferryl forms is demonstrated by the characteristic maxima at 575 nm for  $F^\bullet$  and 607 nm for the  $P_M$  state (Figure 6B). In this case, the loss of 5.1  $\mu$ M of  $F^\bullet$  and 2.7  $\mu$ M  $P_M$  was detected. The average molar amount of lost both ferryl forms ( $[P] + [F^\bullet]$ ) relative to the utilized ferrocyanide was  $0.83 \pm 0.1$  ( $n = 3$ ).

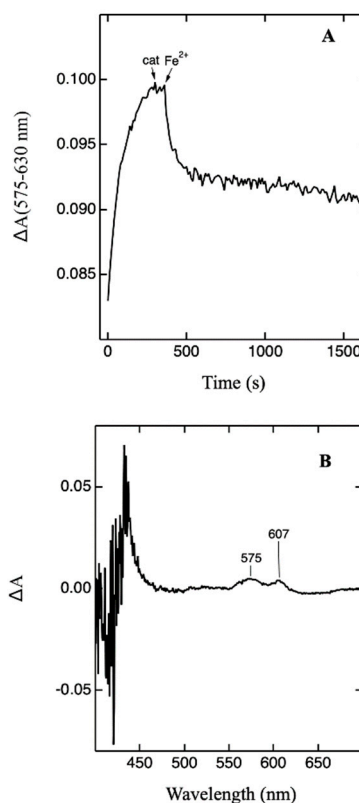
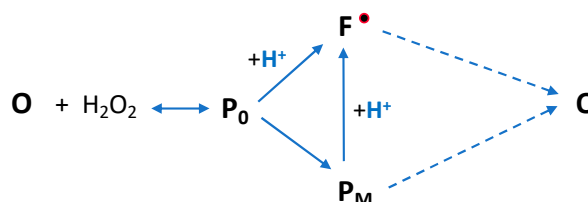


**Figure 6.** One-electron reduction of the  $F^\bullet$  form. (A) Kinetics of the development of the  $F^\bullet$  state from the oxidized CcO ( $49 \mu\text{M}$ ) in the reaction with  $\text{H}_2\text{O}_2$  ( $48 \mu\text{M}$ ) and its reduction by potassium ferrocyanide recorded using the absorbance change  $\Delta A(575\text{--}630 \text{ nm})$ . At times indicated by arrows, the catalase (cat,  $4.7 \mu\text{M}$ ) and ferrocyanide ( $\text{Fe}^{2+}$ ,  $9.9 \mu\text{M}$ ) were injected into the sample. (B) The difference spectrum was calculated between the spectrum collected before and after the addition of ferrocyanide (500s). Conditions of measurement:  $39 \text{ mM}$  potassium phosphate pH 5.7,  $12.5 \text{ mM}$   $\text{K}_2\text{SO}_4$ ,  $7.2 \mu\text{M}$  of oxidized cytochrome *c*, SOD  $300 \text{ units/mL}$ ,  $0.6\%$  DM  $5^\circ\text{C}$ .

### 3. Discussion

The pH-dependent production of two types of ferryl forms in the reaction of the oxidized bovine CcO with a single molecule of  $\text{H}_2\text{O}_2$  has been explained by the following branching Scheme 1 [39,43]:



**Scheme 1.** Reaction of single molecule of  $\text{H}_2\text{O}_2$  with oxidized CcO.

In this scheme, the reversible binding of peroxide into the catalytic center ( $\text{P}_0$  intermediate) is followed by the irreversible redox reaction. The  $\text{P}_0$  intermediate is very likely single or double-ionized hydrogen peroxide bound to heme  $a_3$  forming a non-stable iron-peroxy adduct,  $\text{Fe}_{a_3}^{3+}\text{-O-OH}$  (or  $\text{Fe}_{a_3}^{3+}\text{-O-O}$ ) analogous to compound 0 of peroxidases. At basic pH values dominates the  $\text{P}_0$ -to- $\text{P}_\text{M}$  conversion ( $\text{P}_0 \rightarrow [\text{Fe}_{a_3}^{4+}=\text{O HO-Cu}_\text{B}^{2+} \text{YO}^\bullet]$ ). The transition of the  $\text{P}_0$ -to- $\text{F}^\bullet$ , occurring in acidic solutions, is very likely due to the simultaneous uptake of one proton into the catalytic center ( $\text{P}_0 + \text{H}^+ \rightarrow [\text{Fe}_{a_3}^{4+}=\text{O H}_2\text{O-Cu}_\text{B}^{2+} \text{YO}^\bullet]$ ) [39,43]. It means that both the  $\text{P}_\text{M}$  and the  $\text{F}^\bullet$  forms should be two oxidizing equivalents above the oxidized CcO. In the absence of external electron donors,

these two ferryl states relax very slowly to the apparent oxidized CcO by the autoxidation of the enzyme [55,57,62,63].

The obtained data are in the agreement with the formation of a radical in the peroxide-produced  $F^\bullet$  state. More importantly, the results indicate that the lifetime of the primary  $YO^\bullet$  radical in the  $F^\bullet$  is much shorter than that of the ferryl  $Fe_{a_3}^{4+}=O$  iron. At the time when the ferryl heme  $a_3$  state is developed, the radical in the catalytic center is almost fully quenched. This conclusion is substantiated by three different experimental observations: the enthalpy changes, the EPR detection of the radical, and the reduction of the  $F^\bullet$  form.

The first indication is the large enthalpy change ( $-39$  kcal/mol) associated with the  $O$ -to- $F^\bullet$  transition contrasting with that of the generation of compound I of HRP ( $-27$  kcal/mol) (Figure 4). In the reaction of the oxidized CcO and HRP with  $H_2O_2$ , the measured  $\Delta H$  values can be attributed to two identical events: one is the reversible  $H_2O_2$  binding to the oxidized heme iron and the other is the redox reaction. The earlier investigations of the peroxide binding to the different oxidized heme proteins, employing the mutant of human myoglobin (His64Gly) [64], Mn-reconstituted myoglobin [65], horseradish peroxidase at subzero temperatures [66], and Mn-reconstituted horseradish peroxidase [67], revealed only a small positive  $\Delta H$  with the values between zero and  $+4$  kcal/mol  $H_2O_2$ .

Accordingly, the measured large negative  $\Delta H$  values can be attributed mostly to the redox reactions ( $P_0 \rightarrow [Fe^{4+}=O R^\bullet]$ ). However, from these two heme proteins we know only for the compound I of HRP that both the ferryl iron and  $\pi$ -cation radical are present and very much stable during the ITC measurements. Then the measured  $\Delta H$  of  $-27$  kcal/mol represents the generation of the  $[Fe^{4+}=O R^\bullet]$  state without the contribution of possible side reactions. Because of the similarity of the reactions and the reduction potentials of the ferryl iron and radical in both proteins [10,60,68–70] it may be also expected a similar value of  $\Delta H$  for the production of the  $F^\bullet$  state. Consequently, the excess heat released during the production of the apparent  $F^\bullet$  state ( $-39$  kcal/mol) implicates some additional reaction (s).

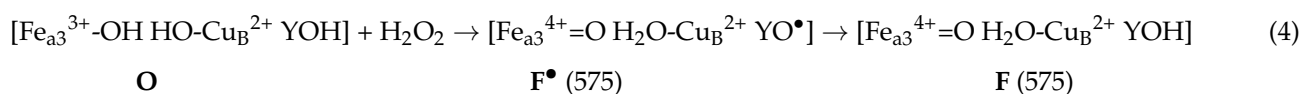
Multiple experimental observations indicate that the side reaction (s) responsible for the excess heat liberated during the generation of the  $F^\bullet$  state is very likely the radical migration and its quenching. This explanation is supported by the observations of the different types and amounts of radicals [37,51–54] when the oxidized CcO was reacted with excess  $H_2O_2$ . More importantly, it has been shown by the EPR spin-trapping technique that  $H_2O_2$  interaction with the catalytic center of the oxidized CcO leads to the appearance of the cysteine thiyl radical [58] and lipid-based radical [63]. Similarly, the spin-trapping using CcO/organic hydroperoxides system documented the protein-centered radical and possible participation of the surface-positioned Tyr, Trp, and Cys residues in its migration [59]. The large distance translocation of the radical,  $30$ – $60$  Å from the heme  $a_3$ - $Cu_B$  center, is corroborated by the modification of several distant Trp residues and bound phospholipids in the  $H_2O_2$ /CcO system [55–57]. The radical migration through the protein matrix is very likely facilitated by ‘wires’ composed of aromatic amino acid residues [56,71].

Secondly, the parallel visible absorption and EPR measurements uncovered only a very small amount of the free radical ( $\sim 0.6\%$ ) relative to the formed  $F^\bullet$  state (Figure 5). This amount is even smaller than previously reported ( $5$ – $20\%$ ) for bovine CcO [37,51,53,54]. This difference can be understood since the nature and the amount of the radical is dependent on the concentration of  $H_2O_2$ , pH of solutions, and very likely also on the reaction time [37,39,50,51,53]. Typically, two overlapping radical signals are observed, one described with a line width of  $45$  G and another with a width of  $12$  G. These two signals have been recently assigned to two Tyr radicals. Narrow one to Tyr244, covalently bound to His240 (ligand of  $Cu_B$ ), and the second to Tyr129 located in the proximity of this center ( $\sim 10$  Å) [53,54]. However, the observed radical in this work showing  $g = 2.005$  and the line width of  $\sim 28$  G cannot be attributed to the combination of the  $45$  and  $12$  G-signals. It seems that this radical is composed of two derivative-like signals: one belongs to the previously detected  $12$  G and the other is characterized by the width of  $\sim 30$  G. Identity of the broader signal is presently not certain.

The kinetics of the appearance of the radical ( $\tau = \sim 200$  s) does not correlate with the generation of the  $F^\bullet$  state (Figure 5, Table 1). The appearance of the radical is, however, closer to the kinetics of the conversion of the small fraction of  $P_M$ -to- $F^\bullet$  state (slow phase,  $\tau = \sim 330$  s) (Figure 5, Table 1). Previously, the kinetics of the conversion of the  $P_M$ -to- $F^\bullet$  was found to correlate with the appearance of a small amount of the radical [51]. In this earlier work, the  $P_M$  state was produced by the reaction of two-electron-reduced CcO with  $O_2$  in a basic buffer, and the  $P_M$ -to- $F^\bullet$  conversion was initiated by the rapid acidification of the solution. The observed radical was attributed to the species formed by the migration of the primary radical from the catalytic center of CcO.

It is believed that the missing detection of the radical in either the  $F^\bullet$  or the  $P_M$  states should be a consequence of the nearby metal ions ( $Fe_{a3}^{4+}=O$ ,  $Cu_B^{2+}$ ). The spin coupling of the radical with  $Cu_B^{2+}$  or the broadening of the radical signal by the interaction with these paramagnetic centers could be a reason for its absence in the EPR spectrum [37,51,72]. Another possibility, indicated by several earlier studies [55–59] together with the present work, is that the primary radical is unstable and can migrate to the surface of the protein and be quenched or captured by spin traps.

Our third approach, a verification of the redox state of the  $F^\bullet$  form, corroborates the rapid migration of the primary radical and its quenching (Figure 6). The reduction of the  $F^\bullet$  state by the sub-stoichiometric amount of ferrocyanide showed that the molar ratio of the lost  $F^\bullet$  along with the  $P_M$  state ( $[F^\bullet] + [P_M]$ ) to the used ferrocyanide is close to one ( $0.83 \pm 0.1$ ). If both the  $F^\bullet$  and the  $P_M$  were two oxidizing equivalents above the  $O$  then this ratio should be 0.5. The result demonstrates that at the time of examination, one-electron reduction of any of these two ferryl intermediates leads to the formation of the oxidized CcO. This time-dependent process is summarized in this scheme:



where the reaction of  $O$  with one molecule of  $H_2O_2$  generates the  $F^\bullet$  state having the ferryl iron of heme  $a_3$  together with the radical, probably Tyr244, at the catalytic center. In the absence of external electron donors, the formation of  $F^\bullet$  is followed by the autoxidation of the enzyme that results in more rapid quenching of the radical ( $YO^\bullet$ ). However, the quenching of radical and production of the  $F$  state are not associated with observable changes in the optical spectrum. Thus, the prepared sample is a mixture of  $F^\bullet$  and  $F$  states showing the maximum at 575 nm and whose composition is dependent on the reaction time.

The data showed that the maxima at 575 nm and 580 nm in the difference spectra of the  $F^\bullet$  and  $F$ , respectively, [37,39] are not caused by the presence or absence of radicals at the catalytic center. We have noticed that the maximum at 575 nm results from the pH dependence of the spectrum of the oxidized CcO [73] utilized in the calculation of the difference spectrum. If the spectrum of the oxidized CcO at pH 8.0 is substituted into this calculation ( $F^\bullet$ - $O$ ), the maximum at  $\sim 580$  nm is observed.

The rate of the radical quenching at the catalytic site in CcO can be estimated from its absence at the time when the  $F^\bullet$  form is developed (Figure 6). Since the formation of the  $Fe_{a3}^{4+}=O$  state in the  $F^\bullet$  form takes place with the time constant of  $\sim 90$  s, then the radical quenching should be at least ten times faster. Consequently, the radical will be lost if its quenching will occur with a time constant of at least less than 9 s (pH 5.7, 5 °C).

The behavior of the primary radical in the  $F^\bullet$ , a shorter lifetime relative to the ferryl iron, is very the same as that what we have recently observed for the radical in the  $P_M$  form at pH 8.0 [74,75]. We have found that the  $P_M$  form is converted with elapsed time to the spectrally similar  $P_R$  form with no radical at the catalytic center [74,75].

The instability of the primary radical in the ferryl  $F^\bullet$  and  $P_M$  forms of CcO is, however, not exceptional among the heme proteins. Such behavior of the radical is very analogous

to that of the primary radicals in myoglobins [76–80], hemoglobins [79–82], cytochrome *c* peroxidase [83], ascorbate peroxidase [84], and prostaglandin H synthase [85].

Ultimate intrinsic electron donors of electrons for the reduction of radicals appear to be Trp residues and phospholipids bound to the purified CcO [55,56,63]. The oxidation of Trp residues and lipids to conjugated dienes and trienes initiated by the reaction of H<sub>2</sub>O<sub>2</sub> with the catalytic center of oxidized CcO has been demonstrated. Cys [58] and Met residues, with midpoint potentials around –250 mV, may also serve as a source of electrons.

The radical migration to the surface of the ferryl form also brings a new explanation for the release of superoxide when oxidized CcO is reacted with an excess of H<sub>2</sub>O<sub>2</sub> [38,45]. Since the production of superoxide was inhibited by the binding of cyanide to the Fe<sub>a3</sub>-Cu<sub>B</sub> center it was assumed that O<sub>2</sub><sup>•–</sup> is released by the direct reduction of the radical at the catalytic center by peroxide. However, the production of O<sub>2</sub><sup>•–</sup> can be also explained by the reaction of H<sub>2</sub>O<sub>2</sub> with the radical migrated to the surface of the ferryl intermediate. In this case, the binding of cyanide to the catalytic center of CcO will also prevent the production of superoxide. For additional confirmation of the rapid radical migration from the catalytic center to the surface of the enzyme, the EPR spin-trapping technique will be employed.

## 4. Materials and Methods

### 4.1. Materials

Potassium phosphate monobasic and dibasic, potassium hydroxide, potassium ferricyanide, potassium ferrocyanide, potassium sulfate, potassium cyanide, horse heart cytochrome *c*, superoxide dismutase (SOD), horseradish peroxidase type VI A, and catalase from bovine liver were purchased from Sigma-Aldrich, Triton X-100 (TX) was from Roche Diagnostics, dodecyl maltoside (DM) from Anatrace, Sepharose Q fast flow from Pharmacia Uppsala and hydrogen peroxide solution (~30%) was from Fluka.

Bovine heart cytochrome *c* oxidase was isolated from mitochondria following the modified method [86] into 10 mM Tris, pH 7.6, 50 mM K<sub>2</sub>SO<sub>4</sub>, and 0.1% TX. To change TX for DM detergent, the purified enzyme was diluted and reconcentrated using microfilters (YM 100, Millipore, cut-off 100 kDa) with the buffer containing 0.1% DM.

Isolated CcO was frozen in liquid nitrogen and stored at –80 °C. The concentration of CcO was determined from the UV-Vis absorption spectrum of the oxidized enzyme using an extinction coefficient  $\epsilon$  (424 nm) = 156 mM<sup>–1</sup>cm<sup>–1</sup> and  $\epsilon$  (428 nm) = 169 mM<sup>–1</sup>cm<sup>–1</sup> for the cyanide-ligated CcO (CcO.CN) [87].

### 4.2. Preparation of Oxidized CcO

The purified CcO may contain some small fractions of a partially reduced enzyme. To obtain the fully oxidized CcO the isolated enzyme (150–200  $\mu$ M) was incubated with 10 mM ferricyanide for 10 min at room temperature. The samples were then passed through a desalting PD-10 column utilizing 5 mM potassium phosphate buffer (KPi), 50 mM K<sub>2</sub>SO<sub>4</sub>, pH 8.0 containing 0.1% DM.

The CcO.CN complex, without free cyanide in the solution, was produced in 20 min. incubations of the purified CcO with 10 mM KCN at 4 °C followed by the addition of 10 mM ferricyanide. This sample was desalted on the PD 10 column 600 s after the addition of ferricyanide as it is described above.

### 4.3. Isothermal Titration Calorimetry (ITC) Measurements

The enthalpy changes ( $\Delta H$ ) associated with the formation of the F<sup>•</sup> state of CcO and compound I of horseradish peroxidase (HRP) were measured by the ITC method during the reaction of the oxidized proteins with sub- and stoichiometric concentrations of H<sub>2</sub>O<sub>2</sub>. The ITC cell was filled with the oxidized protein (~5  $\mu$ M HRP and ~50  $\mu$ M CcO) and the reaction was initiated by a single injection of peroxide (5  $\mu$ M, final concentration). The same buffer was used for the protein in the cell and H<sub>2</sub>O<sub>2</sub> in the injection syringe. Typically, 1.3  $\mu$ L of H<sub>2</sub>O<sub>2</sub> was injected into the cell in 2 s. The measurements were performed in a MicroCal ITC 200 (GE) instrument at the temperature of 5 °C.

The heat linked with the non-specific reactions that could take place in the course of the formation of the  $F^\bullet$  state of CcO was assessed by the injection of  $H_2O_2$  into the cell filled with the oxidized CcO ligated with cyanide. The bound cyanide at the catalytic  $Fe_{a3}-Cu_B$  center of CcO blocks the production of the ferryl state. These control measurements were carried out under identical conditions as those used for the determination of the  $\Delta H$  during the reaction of the oxidized protein with  $H_2O_2$ . Dilution and mixing heat ( $\sim 3\text{--}6\%$  of the total  $\Delta H$ ) were subtracted from the measured reaction enthalpies.

In all experiments in this study, potassium phosphate buffer was used because of its low ionization enthalpies which were important for the measurements of reaction enthalpies by ITC. The temperature of  $5^\circ\text{C}$  was selected in these measurements to decelerate the formation of the  $F^\bullet$  state and to increase the stability of the radical in this form.

#### 4.4. UV-Vis Absorption Spectroscopy Measurements

The formation of the  $F^\bullet$  state, its spontaneous decay, and as well the reduction of this form by ferrocyanide was monitored by visible absorption spectroscopy. The spectral changes induced by the addition of peroxide to oxidized CcO were registered in the diode array spectrometer (Specord S600) at  $5^\circ\text{C}$ . The spectra were recorded in the range of  $400\text{--}700\text{ nm}$  every  $10\text{ s}$  for the first  $600\text{ s}$  and every  $20\text{ s}$  for the next  $3 \times 10^3\text{--}6 \times 10^3\text{ s}$ . From the accumulated spectra the kinetics of the absorbance changes at certain wavelengths and the spectra at the given reaction time was attained.

The reaction of the oxidized CcO with one molecule of  $H_2O_2$  at acidic buffers results in the production mostly of the  $F^\bullet$  form as well as a transient and minor population of the  $P_M$  state. The concentrations of these two ferryl intermediates were calculated from the difference spectrum of the peroxide-treated CcO minus the oxidized CcO employing  $\Delta\epsilon$  ( $607\text{--}630\text{ nm}$ ) =  $11\text{ mM}^{-1}\text{cm}^{-1}$  for the  $P_M$  [88]. Since the  $P_M$  makes also a contribution to the absorbance change  $\Delta A$  ( $575\text{--}630$ ), the measured value was corrected using  $\Delta\epsilon$  ( $575\text{--}630\text{ nm}$ ) =  $2.1\text{ mM}^{-1}\text{cm}^{-1}$ . After this subtraction, the concentration of the  $F^\bullet$  was calculated using  $\Delta\epsilon$  ( $575\text{--}630\text{ nm}$ ) =  $5.3\text{ mM}^{-1}\text{cm}^{-1}$  [88].

The transient rise and the subsequent decay, representing the formation and the decomposition of the ferryl states and the radical, were fitted by the two-step  $A \rightarrow B \rightarrow C$  model:



using equation  $B = A_0((k_1/(k_2 - k_1))(e^{-k_1t}/e^{-k_2t}))$ . Where  $k_1$  and  $k_2$  are corresponding rate constants and  $A_0$  is the initial concentration of the enzyme participating in the reaction.

Extinction coefficient  $\epsilon$  ( $240\text{ nm}$ ) =  $0.04\text{ mM}^{-1}\text{cm}^{-1}$  was utilized to determine the concentration of  $H_2O_2$  [89] and  $\epsilon$  ( $420\text{ nm}$ ) =  $1\text{ mM}^{-1}\text{cm}^{-1}$  of ferricyanide [90]. The concentration of ferrocyanide was established by the oxidation of ferrocyanide to ferricyanide by  $KMnO_4$ . From the spectrum of the produced ferricyanide, the concentration of ferrocyanide was calculated.

#### 4.5. EPR Spectroscopy

The EPR spectra were collected on the frozen samples of  $98\text{ }\mu\text{M}$  oxidized CcO reacted with  $98\text{ }\mu\text{M}$   $H_2O_2$  at  $5^\circ\text{C}$  in  $100\text{ mM}$  phosphate buffer,  $\text{pH } 5.7$ , containing  $30\text{ mM}$   $K_2SO_4$ ,  $0.6\%$  DM, and  $267\text{ units/mL}$  of SOD. After the addition of peroxide to CcO, the aliquots ( $\sim 0.3\text{ mL}$ ) were taken at a certain time from the incubated stock solution and frozen rapidly in a methanol/dry ice bath, and then transferred to liquid nitrogen. These samples were stored in liquid nitrogen until the measurements were performed.

The measurements were carried out in Bruker Elex Sys E500 spectrometer at  $80\text{ K}$  using microwave power of  $0.2\text{ mW}$ . Other parameters of the measurements were: microwave frequency  $9.39\text{ GHz}$ , modulation amplitude  $10\text{ G}$ , modulation frequency  $100\text{ kHz}$ , and time constant  $164 \times 10^{-3}\text{ s}$ .

The generation of the  $F^\bullet$  state from the oxidized CcO (Figure 3), the ITC measurements (Figure 4), and the reduction of the  $F^\bullet$  form by ferrocyanide (Figure 6) represent the typical outcome of three measurements in each case. The EPR examination of the radical in the  $F^\bullet$  form shown in Figure 5 is representative of two measurements.

## 5. Conclusions

In this work, the redox state of the catalytic heme  $a_3$ -Cu<sub>B</sub> center of the peroxide-produced  $F^\bullet$  ferryl form of bovine CcO and the stability of the formed radical in this form were investigated for the first time. The comparison of the heats liberated during the formation of the  $F^\bullet$  in the reaction of the oxidized CcO with H<sub>2</sub>O<sub>2</sub> and that of the compound I of horseradish peroxidase indicates the creation of a radical at heme  $a_3$ -Cu<sub>B</sub> center. However, the primary radical in the  $F^\bullet$  state, plausibly Tyr244, exhibits a much shorter lifetime ( $\tau \leq 9$  s) relative to the rate of the production of the accompanying ferryl iron of heme  $a_3$  ( $\tau = \sim 90$  s). The EPR data, the large enthalpy changes, and the reduction of the  $F^\bullet$  form by the defined amount of ferrocyanide showed that the migration of the radical from the catalytic center is associated with its rapid quenching, very likely at the surface of the protein.

**Author Contributions:** Conceptualization, D.J. and M.F.; Formal analysis, T.S., D.J. and M.F.; Funding acquisition, M.F.; Investigation, T.S., A.T., E.C., D.J. and M.F.; Methodology, E.C., D.J. and M.F.; Project administration, M.F.; Resources, E.C.; Writing—original draft, M.F.; Writing—review & editing, D.J.. All authors have read and agreed to the published version of the manuscript.

**Funding:** This work was supported by the Slovak Grant Agencies (VEGA 1/0028/22) and (APVV-18-0016) and the project “Open scientific community for modern interdisciplinary research in medicine (OPENMED)-ITMS2014+: 313011V455” from the Operational Program Integrated Infrastructure funded by the ERDF.

**Informed Consent Statement:** No humans are involved in this study.

**Data Availability Statement:** Data are presented in this manuscript.

**Acknowledgments:** We would like to thank A. Kliuikov for the assistance during the EPR measurements.

**Conflicts of Interest:** The authors declare no conflict of interest.

## Abbreviations

CcO—cytochrome *c* oxidase, CcO.CN—cyanide ligated cytochrome *c* oxidase, ITC—isothermal titration calorimetry, Fe<sub>a</sub>—iron of heme *a*, Fe<sub>a3</sub>—iron of heme  $a_3$ , TX—Triton X-100, DM—dodecyl maltoside.

## References

1. Sousa, F.L.; Alves, R.J.; Ribeiro, M.A.; Pereira-Leal, J.B.; Teixeira, M.; Manuela, M.; Pereira, M.M. The superfamily of heme–copper oxygen reductases: Types and evolutionary considerations. *Biochim. Biophys. Acta* **2012**, *1817*, 629–637. [[CrossRef](#)] [[PubMed](#)]
2. Pan, L.P.; Hibdon, S.; Liu, R.Q.; Durham, B.; Millett, F. Intracomplex electron transfer between ruthenium-cytochrome *c* derivatives and cytochrome *c* oxidase. *Biochemistry* **1993**, *32*, 8492–8498. [[CrossRef](#)]
3. Szundi, I.; Cappuccio, J.A.; Borovok, N.; Kotlyar, A.B.; Einarsdottir, O. Photoinduced electron transfer in the cytochrome *c*/cytochrome *c* oxidase complex using thiouredopyrenetrisulfonate-labeled cytochrome *c* optical multichannel detection. *Biochemistry* **2001**, *40*, 2186–2193. [[CrossRef](#)]
4. Geren, L.; Durham, B.; Millett, F. Use of Ruthenium Photoreduction Techniques to Study Electron Transfer in Cytochrome Oxidase. *Method Enzym.* **2009**, *456*, 507–520.
5. Ferguson-Miller, S.; Babcock, G.T. Heme/Copper Terminal Oxidases. *Chem. Rev.* **1996**, *96*, 2889–2908. [[CrossRef](#)]
6. Belevich, I.; Verkhovsky, M.I. Molecular mechanism of proton translocation by cytochrome *c* oxidase. *Antio. Redox Sig.* **2008**, *10*, 1–29. [[CrossRef](#)] [[PubMed](#)]
7. Konstantinov, A.A. Cytochrome *c* oxidase: Intermediates of the catalytic cycle and their energy-coupled interconversion. *FEBS Lett.* **2012**, *586*, 630–639. [[CrossRef](#)]
8. Yoshikawa, S.; Shimada, A. Reaction mechanism of cytochrome *c* oxidase. *Chem. Rev.* **2015**, *115*, 1936–1989. [[CrossRef](#)]

9. Rich, P.R. Mitochondrial cytochrome c oxidase: Catalysis, coupling and controversies. *Biochem. Soc. Trans.* **2017**, *45*, 813–829. [[CrossRef](#)]
10. Wikstrom, M.; Krab, K.; Sharma, V. Oxygen Activation and Energy Conservation by Cytochrome c Oxidase. *Chem. Rev.* **2018**, *118*, 2469–2490. [[CrossRef](#)] [[PubMed](#)]
11. Proshlyakov, D.A.; Pressler, M.A.; DeMaso, C.; Leykam, J.F.; DeWitt, D.L.; Babcock, G.T. Oxygen activation and reduction in respiration: Involvement of redox-active tyrosine 244. *Science* **2000**, *290*, 1588–1591. [[CrossRef](#)] [[PubMed](#)]
12. Gorbikova, I.E.A.B.; Wikstrom, M.; Verkhovskiy, M.I. The proton donor for OO bond scission by cytochrome c oxidase. *Proc. Natl. Acad. Sci. USA* **2008**, *105*, 10733–10737. [[CrossRef](#)] [[PubMed](#)]
13. Proshlyakov, D.A.; Pressler, M.A.; Babcock, G.T. Dioxygen activation and bond cleavage by mixed-valence cytochrome c oxidase. *Proc. Natl. Acad. Sci. USA* **1998**, *95*, 8020–8025. [[CrossRef](#)] [[PubMed](#)]
14. Fabian, M.; Wong, W.W.; Gennis, R.B.; Palmer, G. Mass spectrometric determination of dioxygen bond splitting in the “peroxy” intermediate of cytochrome c oxidase. *Proc. Natl. Acad. Sci. USA* **1999**, *96*, 13114–13117. [[CrossRef](#)] [[PubMed](#)]
15. Pinakoulaki, E.; Daskalakis, V.; Ohta, T.; Richter, O.M.; Budiman, K.; Kitagawa, T.; Ludwig, B.; Varotsis, C. The protein effect in the structure of two ferryl-oxo intermediates at the same oxidation level in the heme copper binuclear center of cytochrome c oxidase. *J. Biol. Chem.* **2013**, *288*, 20261–20266. [[CrossRef](#)]
16. Morgan, J.E.; Verkhovskiy, M.I.; Wikstrom, M. Observation and assignment of peroxy and ferryl intermediates in the reduction of dioxygen to water by cytochrome c oxidase. *Biochemistry* **1996**, *35*, 12235–12240. [[CrossRef](#)]
17. Morgan, J.E.; Verkhovskiy, M.I.; Palmer, G.; Wikstrom, M. Role of the P-R intermediate in the reaction of cytochrome c oxidase with O<sub>2</sub>. *Biochemistry* **2001**, *40*, 6882–6892. [[CrossRef](#)]
18. Ishigami, I.; Lewis-Ballester, A.; Echelmeier, A.; Brehm, G.; Zatspein, N.A.; Grant, T.D.; Coe, J.D.; Lisova, S.; Nelson, G.; Zhang, S.; et al. Snapshot of an oxygen intermediate in the catalytic reaction of cytochrome c oxidase. *Proc. Natl. Acad. Sci. USA* **2019**, *116*, 3572–3577. [[CrossRef](#)] [[PubMed](#)]
19. Poiana, F.; von Ballmoos, C.; Gonska, N.; Blomberg, M.R.A.; Adelroth, P.; Brzezinski, P. Splitting of the O-O bond at the heme-copper catalytic site of respiratory oxidases. *Sci. Adv.* **2017**, *3*, e1700279. [[CrossRef](#)]
20. Verkhovskiy, J.E.M.M.I.; Wikstrom, M. Redox transitions between oxygen intermediates in cytochrome-c oxidase. *Proc. Natl. Acad. Sci. USA* **1996**, *93*, 12235–12239. [[CrossRef](#)]
21. Siletsky, A.D.K.S.; Konstantinov, A.A. Resolution of Electrogenic Steps Coupled to Conversion of Cytochrome c Oxidase from the Peroxy to the Ferryl–Oxo State. *Biochemistry* **1999**, *38*, 4853–4861. [[CrossRef](#)] [[PubMed](#)]
22. Verkhovskiy, M.I.J.A.; Verkhovskaya, M.L.; Morgan, J.E.; Wikstrom, M. Proton translocation by cytochrome c oxidase. *Nature* **1999**, *400*, 480–483. [[CrossRef](#)] [[PubMed](#)]
23. Bloch, D.; Belevich, I.; Jasaitis, A.; Ribacka, C.; Puustinen, A.; Verkhovskiy, M.I.; Wikstrom, M. The catalytic cycle of cytochrome c oxidase is not the sum of its two halves. *Proc. Natl. Acad. Sci. USA* **2004**, *101*, 529–533. [[CrossRef](#)] [[PubMed](#)]
24. Faxen, K.; Gilderson, G.; Adelroth, P.; Brzezinski, P. A mechanistic principle for proton pumping by cytochrome c oxidase. *Nature* **2005**, *437*, 286–289. [[CrossRef](#)]
25. Belevich, I.V.; Wikstrom, M.I. Proton-coupled electron transfer drives the proton pump of cytochrome c oxidase. *Nature* **2006**, *440*, 829–832. [[CrossRef](#)]
26. Siletsky, D.H.S.A.; Brand, S.; Morgan, J.E.; Fabian, M.; Geren, L.; Millett, F.; Durham, B.; Konstantinov, A.A.; Gennis, R.B. Single-electron photoreduction of the PM intermediate of cytochrome c oxidase. *Biochim. Biophys. Acta* **2006**, *1757*, 1122–1132. [[CrossRef](#)]
27. Siletsky, S.A.; Gennis, R.B. Time-resolved electrometric: Study of the F→O transition in cytochrome c oxidase. The effect of Zn<sup>2+</sup> ions on the positive side of the membrane. *Biochemistry* **2021**, *86*, 105–122.
28. Zaslavsky, D.; Sadoski, R.C.; Rajagukguk, S.; Geren, L.; Millett, F.; Durham, B.; Gennis, R.B. Direct measurement of proton release by cytochrome c oxidase in solution during the F→O transition. *Proc. Natl. Acad. Sci. USA* **2004**, *101*, 10544–10547. [[CrossRef](#)]
29. Zaslavsky, A.D.K.D.; Smirnova, I.A.; Vygodina, T.; Konstantinov, A.A. Flash-induced membrane potential generation by cytochrome c oxidase. *FEBS Lett* **1993**, *336*, 389–393.
30. Adelroth, M.S.E.P.; Mitchell, D.M.; Gennis, R.B.; Brzezinski, P. Glutamate 286 in Cytochrome aa<sub>3</sub> from *Rhodobacter sphaeroides* Is Involved in Proton Uptake during the Reaction of the Fully-Reduced Enzyme with Dioxygen. *Biochemistry* **1997**, *36*, 13824–13829. [[CrossRef](#)]
31. Verkhovskiy, J.E.M.M.I.; Verkhovskaya, M.; Wikstrom, M. Translocation of electrical charge during a single turnover of cytochrome-c oxidase. *Biochim. Biophys. Acta* **1997**, *1318*, 6–10. [[CrossRef](#)]
32. Adelroth, M.E.P.; Brzezinski, P. Factors determining electron-transfer rates in cytochromecoxidase: Investigation of the oxygen reaction in the R. Sphaeroides enzyme. *Biochim. Biophys. Acta* **1998**, *1367*, 107–117.
33. Jasaitis, M.I.V.A.; Morgan, J.E.; Verkhovskaya, M.L.; Wikström, M. Assignment and Charge Translocation Stoichiometries of the Major Electrogenic Phases in the Reaction of Cytochrome c Oxidase with Dioxygen. *Biochemistry* **1999**, *38*, 2697–2706. [[CrossRef](#)] [[PubMed](#)]
34. Adelroth, M.K.P.; Gilderson, G.; Tomson, F.L.; Gennis, R.B.; Brzezinski, P. Proton transfer from glutamate 286 determines the transition rates between oxygen intermediates in cytochrome c oxidase. *Biochim. Biophys. Acta* **2000**, *1459*, 533–539. [[CrossRef](#)]
35. Siletsky, A.S.P.S.A.; Weiss, K.; Gennis, R.B.; Konstantinov, A.A. Transmembrane charge separation during the ferryl-oxo → oxidized transition in a nonpumping mutant of cytochrome c oxidase. *J. Biol. Chem.* **2004**, *279*, 52558–52565. [[CrossRef](#)]

36. Weng, L.C.; Baker, G.M. Reaction of hydrogen peroxide with the rapid form of resting cytochrome oxidase. *Biochemistry* **1991**, *30*, 5727–5733. [[CrossRef](#)]
37. Fabian, M.; Palmer, G. The interaction of cytochrome oxidase with hydrogen peroxide: The relationship of compounds P and F. *Biochemistry* **1995**, *34*, 13802–13810. [[CrossRef](#)]
38. Ksenzenko, M.; Vygodina, T.V.; Berka, V.; Ruuge, E.K.; Konstantinov, A.A. Cytochrome oxidase-catalyzed superoxide generation from hydrogen peroxide. *FEBS Lett.* **1992**, *297*, 63–66. [[CrossRef](#)]
39. Junemann, S.; Heathcote, P.; Rich, P.R. The reactions of hydrogen peroxide with bovine cytochrome c oxidase. *Biochim. Biophys. Acta* **2000**, *1456*, 56–66. [[CrossRef](#)]
40. Wrigglesworth, J.M. Formation and reduction of a ‘peroxy’ intermediate of cytochrome c oxidase by hydrogen peroxide. *Biochem. J.* **1984**, *217*, 715–719. [[CrossRef](#)]
41. Vygodina, T.V.; Konstantinov, A.A. H<sub>2</sub>O<sub>2</sub>-induced conversion of cytochrome c oxidase peroxy complex to oxoferryl state. *Ann. N. Y. Acad. Sci.* **1988**, *550*, 124–138. [[CrossRef](#)] [[PubMed](#)]
42. Vygodina, T.; Konstantinov, A. Effect of pH on the spectrum of cytochrome c oxidase hydrogen peroxide complex. *Biochim. Biophys. Acta* **1989**, *973*, 390–398. [[CrossRef](#)]
43. Pecoraro, C.; Gennis, R.B.; Vygodina, T.V.; Konstantinov, A.A. Role of the K-channel in the pH-dependence of the reaction of cytochrome c oxidase with hydrogen peroxide. *Biochemistry* **2001**, *40*, 9695–9708. [[CrossRef](#)] [[PubMed](#)]
44. Brittain, T.; Little, R.H.; Greenwood, C.; Watmough, N.J. The reaction of Escherichia coli cytochrome bo with H<sub>2</sub>O<sub>2</sub>: Evidence for the formation of an oxoferryl species by two distinct routes. *FEBS Lett.* **1996**, *399*, 21–25. [[CrossRef](#)]
45. Konstantinov, A.A.; Capitano, N.; Vygodina, T.V.; Papa, S. pH changes associated with cytochrome c oxidase reaction with H<sub>2</sub>O<sub>2</sub>. Protonation state of the peroxy and oxoferryl intermediates. *FEBS Lett.* **1992**, *312*, 71–74. [[CrossRef](#)]
46. Wikstrom, M. Active site intermediates in the reduction of O<sub>2</sub> by cytochrome oxidase, and their derivatives. *Biochim. Biophys. Acta* **2012**, *1817*, 468–475. [[CrossRef](#)]
47. Shimada, A.; Etoh, Y.; Kitoh-Fujisawa, R.; Sasaki, A.; Shinzawa-Itoh, K.; Hiromoto, T.; Yamashita, E.; Muramoto, K.; Tsukihara, T.; Yoshikawa, S. X-ray structures of catalytic intermediates of cytochrome c oxidase provide insights into its O<sub>2</sub> activation and unidirectional proton-pump mechanisms. *J. Biol. Chem.* **2020**, *295*, 5818–5833. [[CrossRef](#)]
48. MacMillan, F.; Kannt, A.; Behr, J.; Prisner, T.; Michel, H. Direct evidence for a tyrosine radical in the reaction of cytochrome c oxidase with hydrogen peroxide. *Biochemistry* **1999**, *38*, 9179–9184. [[CrossRef](#)]
49. Budiman, K.; Kannt, A.; Lyubenova, S.; Richter, O.M.; Ludwig, B.; Michel, H.; MacMillan, F. Tyrosine 167: The origin of the radical species observed in the reaction of cytochrome c oxidase with hydrogen peroxide in Paracoccus denitrificans. *Biochemistry* **2004**, *43*, 11709–11716. [[CrossRef](#)]
50. von der Hocht, I.; van Wonderen, J.H.; Hilbers, F.; Angerer, H.; MacMillan, F.; Michel, H. Interconversions of P and F intermediates of cytochrome c oxidase from Paracoccus denitrificans. *Proc. Natl. Acad. Sci. USA* **2011**, *108*, 3964–3969. [[CrossRef](#)]
51. Rich, P.R.; Rigby, S.E.; Heathcote, P. Radicals associated with the catalytic intermediates of bovine cytochrome c oxidase. *Biochim. Biophys. Acta* **2002**, *1554*, 137–146. [[CrossRef](#)]
52. Rigby, S.E.; Junemann, S.; Rich, P.R.; Heathcote, P. Reaction of bovine cytochrome c oxidase with hydrogen peroxide produces a tryptophan cation radical and a porphyrin cation radical. *Biochemistry* **2000**, *39*, 5921–5928. [[CrossRef](#)] [[PubMed](#)]
53. Yu, M.A.; Egawa, T.; Shinzawa-Itoh, K.; Yoshikawa, S.; Guallar, V.; Yeh, S.R.; Rousseau, D.L.; Gerfen, G.J. Two tyrosyl radicals stabilize high oxidation states in cytochrome C oxidase for efficient energy conservation and proton translocation. *J. Am. Chem. Soc.* **2012**, *134*, 4753–4761. [[CrossRef](#)] [[PubMed](#)]
54. Yu, M.A.; Egawa, T.; Shinzawa-Itoh, K.; Yoshikawa, S.; Yeh, S.R.; Rousseau, D.L.; Gerfen, G.J. Radical formation in cytochrome c oxidase. *Biochim. Biophys. Acta* **2011**, *1807*, 1295–1304. [[CrossRef](#)] [[PubMed](#)]
55. Musatov, A.; Hebert, E.; Carroll, C.A.; Weintraub, S.T.; Robinson, N.C. Specific modification of two tryptophans within the nuclear-encoded subunits of bovine cytochrome c oxidase by hydrogen peroxide. *Biochemistry* **2004**, *43*, 1003–1009. [[CrossRef](#)]
56. Musatov, A.; Robinson, N.C. Susceptibility of mitochondrial electron-transport complexes to oxidative damage. Focus on cytochrome c oxidase. *Free Radic. Res.* **2012**, *46*, 1313–1326. [[CrossRef](#)]
57. Lemma-Gray, P.; Weintraub, S.T.; Carroll, C.A.; Musatov, A.; Robinson, N.C. Tryptophan 334 oxidation in bovine cytochrome c oxidase subunit I involves free radical migration. *FEBS Lett.* **2007**, *581*, 437–442. [[CrossRef](#)]
58. Chen, Y.R.; Gunther, M.R.; Mason, R.P. An electron spin resonance spin-trapping investigation of the free radicals formed by the reaction of mitochondrial cytochrome c oxidase with H<sub>2</sub>O<sub>2</sub>. *J. Biol. Chem.* **1999**, *274*, 3308–3314. [[CrossRef](#)]
59. Chen, Y.R.; Mason, R.P. Mechanism in the reaction of cytochrome c oxidase with organic hydroperoxides: An ESR spin-trapping investigation. *Biochem. J.* **2002**, *365*, 461–469. [[CrossRef](#)]
60. Hayashi, Y.; Yamazaki, I. The oxidation-reduction potentials of compound I/compound II and compound II/ferric couples of horseradish peroxidases A2 and C. *J. Biol. Chem.* **1979**, *254*, 9101–9106. [[CrossRef](#)]
61. Hewson, W.D.; Hager, L.P. Oxidation of horseradish peroxidase compound II to compound I. *J. Biol. Chem.* **1979**, *254*, 3182–3186. [[CrossRef](#)]
62. Musatov, A. Contribution of peroxidized cardiolipin to inactivation of bovine heart cytochrome c oxidase. *Free Radic. Biol. Med.* **2006**, *41*, 238–246. [[CrossRef](#)] [[PubMed](#)]
63. Jancura, D.; Stanicova, J.; Palmer, G.; Fabian, M. How hydrogen peroxide is metabolized by oxidized cytochrome c oxidase. *Biochemistry* **2014**, *53*, 3564–3575. [[CrossRef](#)]

64. Khan, K.K.; Mondal, M.S.; Padhy, L.; Mitra, S. The role of distal histidine in peroxidase activity of myoglobin—Transient-kinetics study of the reaction of H<sub>2</sub>O<sub>2</sub> with wild-type and distal-histidine-mutanted recombinant human myoglobin. *Eur. J. Biochem.* **1998**, *257*, 547–555. [[CrossRef](#)] [[PubMed](#)]
65. Mondal, M.S.; Mitra, S. Kinetic studies of the two-step reactions of H<sub>2</sub>O<sub>2</sub> with manganese-reconstituted myoglobin. *Biochim. Biophys. Acta* **1996**, *1296*, 174–180. [[CrossRef](#)]
66. Baek, H.K.; Van Wart, H.E. Elementary steps in the formation of horseradish peroxidase compound I: Direct observation of compound 0, a new intermediate with a hyperporphyrin spectrum. *Biochemistry* **1989**, *28*, 5714–5719. [[CrossRef](#)]
67. Khan, K.K.; Mondal, M.S.; Mitra, S. Kinetic studies of the reaction of hydrogen peroxide with manganese-reconstituted horseradish peroxidase. *J. Chem. Soc. Dalton Trans.* **1996**, 1059–1062. [[CrossRef](#)]
68. Farhangrazi, Z.S.; Copeland, B.R.; Nakayama, T.; Amachi, T.; Yamazaki, I.; Powers, L.S. Oxidation-reduction properties of compounds I and II of *Arthromyces ramosus* peroxidase. *Biochemistry* **1994**, *33*, 5647–5652. [[CrossRef](#)] [[PubMed](#)]
69. Blomberg, M.R.A. Active Site Midpoint Potentials in Different Cytochrome c Oxidase Families: A Computational Comparison. *Biochemistry* **2019**, *58*, 2028–2038. [[CrossRef](#)]
70. Siegbahn, P.E.M.; Blomberg, M.R.A. A Systematic DFT Approach for Studying Mechanisms of Redox Active Enzymes. *Front. Chem.* **2018**, *6*, 644. [[CrossRef](#)]
71. Gray, H.B.; Winkler, J.R. Hole hopping through tyrosine/tryptophan chains protects proteins from oxidative damage. *Proc. Natl. Acad. Sci. USA* **2015**, *112*, 10920–10925. [[CrossRef](#)]
72. Watmough, N.J.; Cheesman, M.R.; Greenwood, C.; Thomson, A.J. Cytochrome bo from *Escherichia coli*: Reaction of the oxidized enzyme with hydrogen peroxide. *Biochem. J.* **1994**, *300*, 469–475. [[CrossRef](#)] [[PubMed](#)]
73. Parul, D.; Palmer, G.; Fabian, M. Proton interactions with hemes a and a<sub>3</sub> in bovine heart cytochrome c oxidase. *Biochemistry* **2005**, *44*, 4562–4571. [[CrossRef](#)] [[PubMed](#)]
74. Mikulova, L.; Pechova, I.; Jancura, D.; Stupak, M.; Fabian, M. Thermodynamics of the P-type Ferryl Form of Bovine Cytochrome c Oxidase. *Biochemistry* **2021**, *86*, 74–83. [[CrossRef](#)] [[PubMed](#)]
75. Sztachova, T.; Pechova, I.; Mikulova, L.; Stupak, M.; Jancura, D.; Fabian, M. Peroxide stimulated transition between the ferryl intermediates of bovine cytochrome c oxidase. *Biochim. Biophys. Acta Bioenerg.* **2021**, *1862*, 148447. [[CrossRef](#)] [[PubMed](#)]
76. King, N.K.; Winfield, M.E. The mechanism of metmyoglobin oxidation. *J. Biol. Chem.* **1963**, *238*, 1520–1528. [[CrossRef](#)]
77. Wilks, A.; Ortiz de Montellano, P.R. Intramolecular translocation of the protein radical formed in the reaction of recombinant sperm whale myoglobin with H<sub>2</sub>O<sub>2</sub>. *J. Biol. Chem.* **1992**, *267*, 8827–8833. [[CrossRef](#)]
78. Tew, D.; Ortiz de Montellano, P.R. The myoglobin protein radical. Coupling of Tyr-103 to Tyr-151 in the H<sub>2</sub>O<sub>2</sub>-mediated cross-linking of sperm whale myoglobin. *J. Biol. Chem.* **1988**, *263*, 17880–17886. [[CrossRef](#)]
79. Svistunenko, D.A. An EPR study of the peroxy radicals induced by hydrogen peroxide in the haem proteins. *Biochim. Biophys. Acta* **2001**, *1546*, 365–378. [[CrossRef](#)]
80. Svistunenko, D.A.; Dunne, J.; Fryer, M.; Nicholls, P.; Reeder, B.J.; Wilson, M.T.; Bigotti, M.G.; Cutruzzola, F.; Cooper, C.E. Comparative study of tyrosine radicals in hemoglobin and myoglobins treated with hydrogen peroxide. *Biophys. J.* **2002**, *83*, 2845–2855. [[CrossRef](#)]
81. Witting, P.K.; Douglas, D.J.; Mauk, A.G. Reaction of human myoglobin and H<sub>2</sub>O<sub>2</sub>. Involvement of a thiyl radical produced at cysteine 110. *J. Biol. Chem.* **2000**, *275*, 20391–20398. [[CrossRef](#)] [[PubMed](#)]
82. Reeder, B.J.; Svistunenko, D.A.; Cooper, C.E.; Wilson, M.T. The radical and redox chemistry of myoglobin and hemoglobin: From in vitro studies to human pathology. *Antioxid. Redox Signal.* **2004**, *6*, 954–966. [[PubMed](#)]
83. Erman, J.E.; Yonetani, T. A kinetic study of the endogenous reduction of the oxidized sites in the primary cytochrome c peroxidase-hydrogen peroxide compound. *Biochim. Biophys. Acta* **1975**, *393*, 350–357. [[CrossRef](#)]
84. Hiner, A.N.; Martinez, J.I.; Arnao, M.B.; Acosta, M.; Turner, D.D.; Lloyd Raven, E.; Rodriguez-Lopez, J.N. Detection of a tryptophan radical in the reaction of ascorbate peroxidase with hydrogen peroxide. *Eur. J. Biochem.* **2001**, *268*, 3091–3098. [[CrossRef](#)]
85. Wu, G.; Rogge, C.E.; Wang, J.S.; Kulmacz, R.J.; Palmer, G.; Tsai, A.L. Oxyferryl heme and not tyrosyl radical is the likely culprit in prostaglandin H synthase-1 peroxidase inactivation. *Biochemistry* **2007**, *46*, 534–542. [[CrossRef](#)]
86. Soulimane, T.; Buse, G. Integral Cytochrome-C-Oxidase—Preparation and Progress Towards a 3-Dimensional Crystallization. *Eur. J. Biochem.* **1995**, *227*, 588–595. [[CrossRef](#)]
87. Liao, G.L.; Palmer, G. The reduced minus oxidized difference spectra of cytochromes a and a(3). *Bba-Bioenergetics* **1996**, *1274*, 109–111. [[CrossRef](#)]
88. Wikstrom, M.; Morgan, J.E. The dioxygen cycle. Spectral, kinetic, and thermodynamic characteristics of ferryl and peroxy intermediates observed by reversal of the cytochrome oxidase reaction. *J. Biol. Chem.* **1992**, *267*, 10266–10273. [[CrossRef](#)]
89. Bergmayer, H.U.; Gawehn, K.; Grassl, M. Methoden der Enzymatischen Analyze. Bergmayer, H.U., Ed.; Verlag Chemie: Weinheim, Germany, 1970; p. 440.
90. Appleby, C.A.; Morton, R.K. Lactic dehydrogenase and cytochrome b2 of baker's yeast; purification and crystallization. *Biochem. J.* **1959**, *71*, 492–499. [[CrossRef](#)] [[PubMed](#)]